Enhanced Hypothalamic Glucose Sensing in Obesity: Alteration of Redox Signaling

Anne-Laure Colombani,[1] Lionel Carneiro,[1] Alexandre Benani,[1] Anne Galinier,[1] Tristan Jaillard,[1] Thibaut Duparc,[1] Géraldine Offer,[1] Anne Lorsignol,[1] Christophe Magnan,[2] Louis Casteilla,[1] Luc Pénicaud,[1] and Corinne Leloup[1]

OBJECTIVE—Recent data demonstrated that glucose sensing in different tissues is initiated by an intracellular redox signaling pathway in physiological conditions. However, the relevance of such a mechanism in metabolic disease is not known. The aim of the present study was to determine whether brain glucose hypersensitivity present in obese Zücker rats is related to an alteration in redox signaling.

RESEARCH DESIGN AND METHODS—Brain glucose sensing alteration was investigated in vivo through the evaluation of electrical activity in arcuate nucleus, changes in reactive oxygen species levels, and hypothalamic glucose-induced insulin secretion. In basal conditions, modifications of redox state and mitochondrial functions were assessed through oxidized glutathione, glutathione peroxidase, manganese superoxide dismutase, aconitase activities, and mitochondrial respiration.

RESULTS—Hypothalamic hypersensitivity to glucose was characterized by enhanced electrical activity of the arcuate nucleus and increased insulin secretion at a low glucose concentration, which does not produce such an effect in normal rats. It was associated with *1*) increased reactive oxygen species levels in response to this low glucose load, *2*) constitutive oxidized environment coupled with lower antioxidant enzyme activity at both the cellular and mitochondrial level, and *3*) overexpression of several mitochondrial subunits of the respiratory chain coupled with a global dysfunction in mitochondrial activity. Moreover, pharmacological restoration of the glutathione hypothalamic redox state by reduced glutathione infusion in the third ventricle fully reversed the cerebral hypersensitivity to glucose.

CONCLUSIONS—The data demonstrated that obese Zücker rats' impaired hypothalamic regulation in terms of glucose sensing is linked to an abnormal redox signaling, which originates from mitochondria dysfunction. ***Diabetes*** **58:2189–2197, 2009**

From the [1]Métabolisme, Plasticité et Mitochondrie, Unité Mixte de Recherche 5241, Centre National de la Recherche Scientifique, Université Paul Sabatier, Toulouse, France; and the [2]Physiopathologie de la Nutrition, Unité Mixte de Recherche 7059, Centre National de la Recherche Scientifique, Université Denis Diderot, Paris, France.

Corresponding author: Corinne Leloup, leloup@cict.fr.

Received 25 January 2009 and accepted 22 June 2009.

Published ahead of print at http://diabetes.diabetesjournals.org on 6 July 2009. DOI: 10.2337/db09-0110.

It is well established that the brain has a critical role in regulating the energy needs of the body (1). Both carbohydrate and lipid stores are monitored by the brain using metabolic, hormonal, and neural signals from the periphery (2,3). These signals enter the brain and trigger neuroendocrine and autonomic responses that maintain energy homeostasis (4,5). Among the metabolic signals, glucose has long been identified and the physiological relevance of hypothalamic glucoresponsive neurons has been directly demonstrated (6). The molecular mechanisms underlying the glucose responsiveness of neurons in the hypothalamus exhibit β-cell analogy involving GLUT2, glucokinase, and K_{ATP} channels (7–10). Recently, a novel signaling pathway involving mitochondrial reactive oxygen species (mROS) was identified (11–13). Both pancreatic and hypothalamic studies pointed to mROS as a necessary signal to initiate the response to "glucose sensing" (e.g., insulin secretion). These studies suggest that a finely controlled mROS production depending on mitochondrial activity might be considered as a master physiological messenger in metabolite-sensitive cells.

Obesity is a major health problem in Western societies coupled with a high risk of developing insulin resistance. Rodent experimental models of obesity display impaired metabolic and hormonal brain sensing (14). Recent work demonstrated that the alteration of the hypothalamic glucose-sensing mechanism was sufficient to induce dramatic effects on energy balance correlated to mitochondrial abnormalities (6,15). Zücker rats exhibit a strong presence of obesity and an insulin resistance with dramatic autonomic disturbances, that is, modification of the sympathovagal balance (16,17). This model is also characterized by cerebral hypersensitivity to glucose, which initiates an abnormal vagus-induced insulin secretion (18,19). In this study, we set out to determine the role of redox signaling in hypothalamic hypersensitivity to glucose in this model of obesity. In addition, hypothalamic electrical activity has been characterized and shown to be correlated to aberrant mROS levels, redox state, and mitochondrial activity. Finally, restoration of the redox state fully reversed the cerebral hypersensitivity to glucose.

RESEARCH DESIGN AND METHODS

Genetically obese (*fa/fa*) and lean (Fa/?) male Zücker rats (7 weeks old; Charles River) were housed in a controlled environment (12-h light/dark cycle, lights on at 7:00 A.M., 22°C) and fed ad libitum (Harlan, Gannat, France). Surgeries and experiments were performed under pentobarbital anesthesia (50 mg/kg, Centravet, Dinan, France) except where noted. All procedures involving rats were in accordance with the European Communities Council

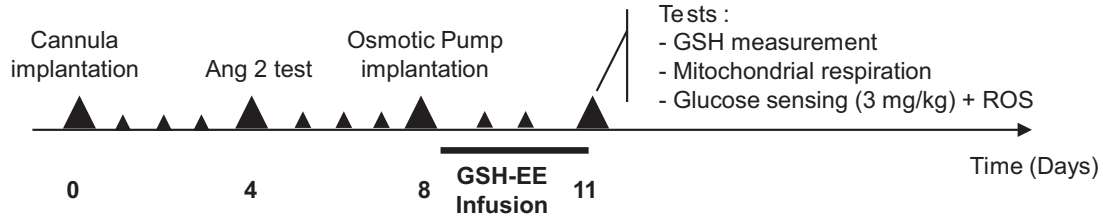

FIG. 1. Schematic representation of experimental procedure for reduced glutathione infusion (GSH-EE, reduced glutathione ethyl ester).

Directive (86/609/EEC) and reviewed by a local committee. All experiments were carried out after a period of 3 h fasting beginning at time of lights on.

Intracarotid injection of glucose toward the brain. A catheter was inserted into the carotid artery and pushed on 5 mm in the cranial direction. A bolus of 3 or 9 mg/kg glucose in 100 μl of adapted saline concentration was injected toward the brain in 30 s. Saline and glucose in saline solutions were equiosmolar (300 mOsm).

Neuronal activity recordings. Multiunit recordings within arcuate were made using a monopolar platinum electrode (Phymep, Paris, France) as previously described (20). Rats were placed in a stereotaxic apparatus (David Kopf), and arcuate nucleus was targeted according to coordinates obtained from Paxinos stereotaxic atlas: −3.1 mm posterior to bregma, −8.7 mm under the brain surface, and 0.4 mm from the midline. Action potentials were displayed and saved on a computer after initial amplification through a low-noise amplifier (BIO amplifier, AD Instrument, Rabalot, France). Data were digitized with a PowerLab/4sp digitizer. Signals were amplified 10^5 and filtered at low and high frequency cutoffs of 100 and 1,000 Hz and monitored with the Chart 4 computer program. Baseline unit activity was recorded for 10 min before infusion of a compound. Multiunit recordings were made in response to a 100 μl intracarotid ipsilateral injection of either saline or glucose.

Osmotic pump implantation. Cannula (Plastics one, Phymep) was targeted to the third ventricle (2.6 mm posterior to the bregma and 10.0 mm below the dura). Four days later, only rats with dipsogenic effects (angiotensin II, 60 pmol, 3 μl; Sigma-Aldrich, St. Quentin Fallavier, France) were used for intracerebroventricular infusions. Four days later, the osmotic minipump (1 μl/h, 3 days, model 1003D; Alzet, Charles River, St. Germain sur l'Arbresle, France) filled either with PBS-HEPES (5 mmol/l) or with glutathione (1 mol/l) (21) (Sigma-Aldrich) was implanted under isoflurane gas anesthesia. Experiments were performed 3 days later (Fig. 1).

Mitochondrial extraction. Animals were killed by cervical dislocation. Brains were removed and immediately immersed in ice-cold PBS-HEPES (5 mmol/l). Dissected tissues were immersed for 15 min in a buffer A (10 mmol/l HEPES, 10 mmol/l KCl, 240 mmol/l sucrose, protease inhibitor cocktail tablet [complete Mini; Roche, Meylan, France]) and homogenized with a dounce homogenizer (7.5 μl/10 mg tissues of buffer A). The homogenate was resuspended in 125 μl/10 mg tissues of buffer A and centrifuged (1,000 × g, 10 min, 4°C). The supernatant was centrifuged (12,000 × g, 10 min, 4°C). The remaining mitochondrial pellet was resuspended either in 8.2 μl/10 mg tissues of buffer B (10 mmol/l HEPES, 420 mmol/l NaCl, 0.5 mmol/l Dithiothreitol, and protease inhibitor cocktail tablet) for Western blot analysis or in 16.5 μl/10 mg tissues of Mitomed R05 solution (0.5 mmol/l EGTA, 60 mmol/l K-Lactobionate, 20 mmol/l Taurine, 10 mmol/l KH_2PO_4, 3 mmol/l $MgCl_2$, 110 mmol/l sucrose, 1 g/l free fatty acid BSA, 20 mmol/l HEPES, and pH = 7.1) for O_2 consumption measurement.

Immunoblotting analysis of respiratory chain complexes. Mitochondrial proteins (10 μg) were separated on SDS-PAGE 15% for OXPHOS immunolabeling, using a cocktail of antibodies that recognizes respiratory chain complexes. After transfer onto a Hybond membrane (Amersham, GE Healthcare, Ramonville, France), blocking was performed for 1 h at room temperature in 5% nonfat milk prepared in Tris-buffered saline with tween 0.2%. Membranes were probed with 1/500 of mouse anti-OXPHOS (Mitosciences, Euromedex, Souffelweyersheim, France) overnight at 4°C. Specific bands of OXPHOS were detected using a goat anti-mouse peroxidase-conjugated secondary antibody (Amersham) revealed with a chemioluminescence kit (Amersham) and exposed to autoradiographic films. Immunolabeled bands were quantified from densitometry analysis.

O_2 consumption measurement on mitochondria. Oxygen consumption was measured using a respirometer (Oxygraph-2k; Oroboros Instruments, Innsbruck, Austria) as previously described (22). Measurements were taken with stirring (750 rpm) in 2 ml of Mitomed R05 at 30°C. The medium was equilibrated with air for 30 min, and mitochondria (200 μg) were transferred into the respirometer's glass chambers. Mitochondrial respiration was stimulated by the successive addition of substrates 1, 5, and 20 mmol/l glutamate to achieve the apparent state 2. Then, 0.1 mmol/l ADP was added to achieve the apparent state 3 respirations. Next, 5 μmol/l carboxy-atractylate (CAtr) was added to block ATP synthesis and achieve the apparent state 4 respiration. Finally, 1 μmol/l potassium cyanide (KCN) was added to obtain the nonmitochondrial O_2 consumption. Mitochondrial states 2, 3, and 4 were calculated by subtracting the nonmitochondrial O_2 consumption from apparent states. The respiratory control ratio (RCR) was the state 3-to-state 4 ratio. Uncoupled respiration was assessed using glutamate (20 mmol/l), CAtr (5 μmol/l), and palmitate (300 μmol/l) stimulation. Carbonyl cyanide *m*-chlorophenylhydrazone (CCCP, 0.4 μmol/l), a chemical uncoupler, was used to measure the maximal respiration. Oxygen consumption was calculated using DataGraph software. Media were prepared according to the guide provided by Oroboros Instruments. Technical sheets are available on the company Web site at http://www.oroboros.at/.

ROS level measurement. One minute after glucose injection, rats were decapitated, brains quickly removed, and hypothalami and thalami dissected on ice-cooled glass plate. Brain areas were immediately frozen in nitrogen liquid and stored at −80°C. ROS were assessed with the 2–7-dichlorofluorescein diacetate probe (23) (Invitrogen, Cergy Pontoise, France) and quantified in a fluorescent plate reader at 535 nm under excitation at 490 nm using a microplate reader (Victor Wallace, Perkin Elmer, Courtaboeuf, France).

Aconitase activity measurement. Maximum aconitase activity measurement was performed using a protocol already described (24). The photochrome was measured at 525 nm using the UVIKON Spectrophotometer 922.

Enzymatic and nonenzymatic antioxidant. Tissue pieces were homogenized in a lysis saline solution (3 mmol/l EDTA, 150 mmol/l KCl, and pH = 7.4). Homogenates (50 μl) mixed with 450 μl of 5% metaphosphoric acid were then centrifuged (1,500 × g, 10 min, 4°C). Final supernatant was used for glutathione and antioxidant enzyme assays. Glutathione assay was performed by reverse-phase high-performance liquid chromatography (HPLC) as previously described (25). Total glutathione (GSx) was the sum of reduced glutathione (GSH) and twofold oxidized glutathione (GSSG) concentrations ([GSx] = [2 × GSSG] + [GSH]). We then calculated the redox state of glutathione as (GSSG/GSx) × 100. Superoxide dimutase (SOD) activity (manganese superoxide dismutase [MnSOD] and Cu/Zn SOD) was assayed using the inhibition of pyrogallol autoxidation (26). One enzymatic unit of SOD activity was defined as the amount of enzyme that inhibited pyrogallol autoxidation by 50%. Glutathione peroxidase (GPx) activity was measured using t-butylhydroperoxide as substrate (27). One enzymatic unit of GPx activity corresponds to the oxidation of 1 mmol of NADPH/min.

Mitochondrial quantification. Citrate synthase assay was measured according to the procedure of Srere (28): one enzymatic unit of citrate synthase was equal to the reduction of 1 mmol of 5–5′-dithiobis-2-nitrobenzoic acid per min.

Cytochrome oxidase activity. Fresh hypothalami were homogenized in cold buffer (0.25 mol/l sucrose, 5 mmol/l TES, and pH = 7.2) and cyclooxygenase activity measured as previously described (29).

Protein assay. Concentration of samples was determined using the DC protein assay kit (Biorad, Marnes la Coquette, France) according to the manufacturer's instructions.

Plasma glucose and insulin concentrations. Plasma was isolated from the blood collected at the rat-tail blood vessels. Glucose and insulin were determined using a glucose analyzer (One Touch II) and an ultrasensitive ELISA kit (Eurobio, Paris, France), respectively.

Statistical analysis. Results are presented as means ± SE. Comparisons between groups were carried out for each parameter using Prism 4.0 software (GraphPad Software). A two-way ANOVA was applied first to detect interactions between genotype and treatment. When genotype did not produce any significant effect, one-way ANOVA was then applied; otherwise, groups were analyzed independently using Student's or Mann-Whitney *U* tests when appropriate. After one-way ANOVA, multiple comparisons of means were further computed with Newman-Keuls test. Both Bartlett's and Shapiro Wilk's tests were also applied to check equality in variance and normality of distribution, respectively. For some parameters, nonparametric Kruskal-Wallis and Mann-Whitney *U* tests were used when appropriate, that is,

TABLE 1
Characteristics of Zücker rats

	Body (g)	Insulinemia (μU/ml)	Glycemia (mM)
Lean	221.50 ± 5.64	26.05 ± 3.26	5.75 ± 0.15
Obese	258.17 ± 7.23***	142.70 ± 2.68	5.96 ± 0.07

Basal values of body weight, insulinemia, and glycemia are expressed as means ± SE (7-week-old rats). Significant differences according to the unpaired Student's t test ($n = 7$) compared with lean littermates. ***$P < 0.001$.

heterogeneity of variances. For single comparison, that is, lean versus obese, nonpaired Student's t test was applied. Significant difference was noted *, **, or *** on the graphic representation when P value was <0.05, 0.01, and 0.001, respectively.

RESULTS

Seven-week-old obese Zücker rats were hyperinsulinemic (142.70 ± 2.68 vs. 26.05 ± 3.26 μU/ml) but normoglycemic (5.96 ± 0.07 vs. 5.75 ± 0.15 mmol/l) (Table 1).

Obese rats exhibit brain hypersensitivity to glucose. We confirmed the cerebral hypersensitivity exhibited by obese rats in response to glucose. Thus, 9 mg/kg glucose injection into the carotid artery toward the brain caused a rapid and transient increase of plasma insulin (50 μU/ml) 1 min after the carotid injection in lean and obese rats (Fig. 2*A*) (18,30). When a similar test was performed with a lower dose of glucose (3 mg/kg), insulin secretion did not occur in lean rats. By contrast, in obese Zücker rats, this lower dose of glucose was sufficient to produce a rapid and transient increase in plasma insulin concentration. Amplitude and delay of this 3 mg/kg glucose-stimulated insulin secretion were similar to those observed with a glucose dose of 9 mg/kg in lean rats ($P = 0.5737$) (Fig. 2*A*). These results demonstrate that obese animals exhibit brain glucose hypersensitivity. This intracarotid glucose injection did not raise systemic glucose levels at any time during the test (Fig. 2*B*). Therefore, the insulin response is only because of cerebral glucose sensing and cannot result from peripheral effects.

Stimulation of multicellular hypothalamic electrical activity at the low glucose dose in obese rats. We previously showed that the activation of extracellular hypothalamic activity in arcuate nucleus in response to glucose was required to initiate insulin secretion in normal rats (12). Here, we explored the effect of 3 mg/kg glucose on extracellular arcuate nucleus electrical activity in both phenotypes. Basal glycemia at the time of recording was 5.91 ± 0.33, 6.05 ± 0.22, 5.89 ± 0.26, and 5.90 ± 0.59 mmol/l for lean and obese NaCl-injected rats and lean and obese 3 mg/kg glucose–injected rats, respectively. In lean rats, 3 mg/kg glucose induced a slight increase in arcuate electrical activity compared with saline injection (33%, $P < 0.01$). It also induced a significant increase in electrical events in obese animals when compared with saline injection (71%, $P < 0.001$) (Fig. 3) that differ significantly from the ones observed in lean rats injected with glucose ($P < 0.01$). Moreover, in contrast to obese rats, 3 mg/kg glucose–induced electrical activity was not associated with insulin secretion in lean rats.

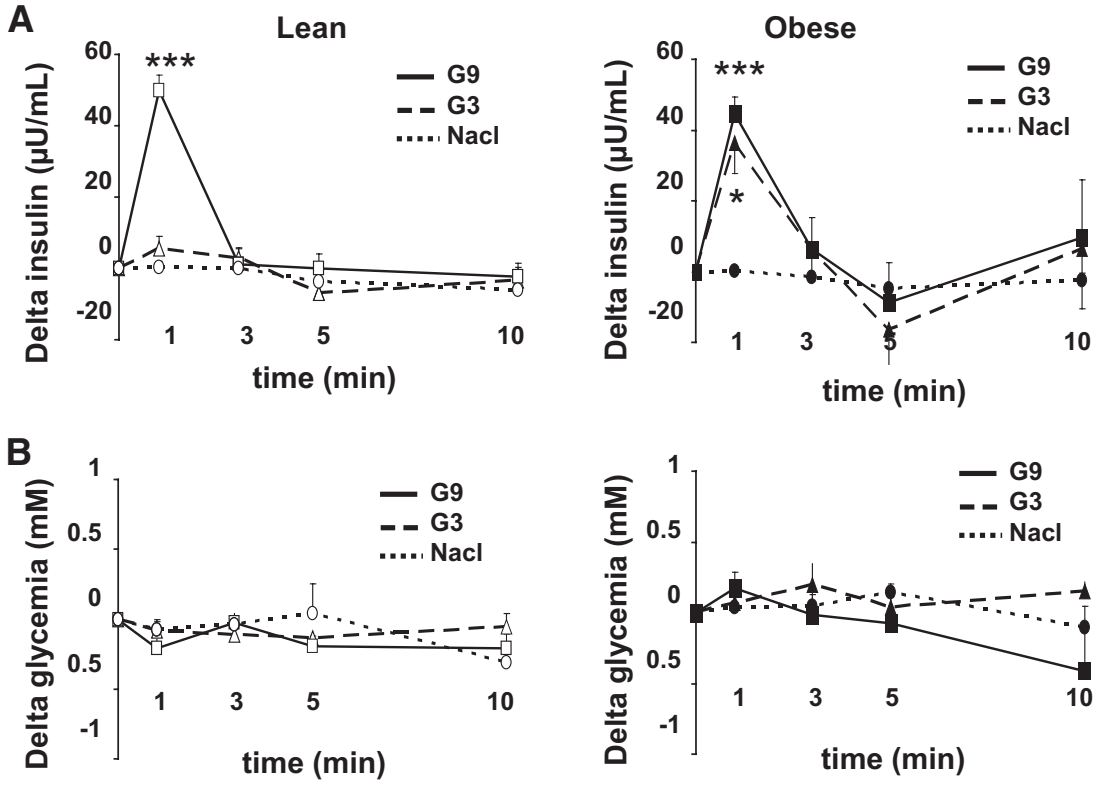

FIG. 2. Hypothalamic hypersensitivity to glucose in the obese Zücker rat. *A*: Insulin secretion in response to glucose. Plasma insulin in obese and lean rats in response to saline (dotted line) or 3 mg/kg (G3, dash line) or 9 mg/kg (G9, black line) glucose injection toward the brain. Results are expressed as means ± SE (Δ from basal insulinemia at $t = 0$). Asterisk indicates significant differences according to independent statistical analysis using Mann-Whitney U test at $t = 1$ min, $n = 6$–9 per genotype (*$P < 0.05$ and ***$P < 0.001$). *B*: No change in glycemia during the glucose-sensing test. Glycemia in response to saline (dotted line) or 3 mg/kg (G3, dash line) or 9 mg/kg (G9, black line) glucose injection toward the brain. Results are expressed as means ± SE (Δ from basal glycemia at $t = 0$). No significant differences were detected using two-way ANOVA analysis at $t = 1$ min ($n = 6$–9 per genotype).

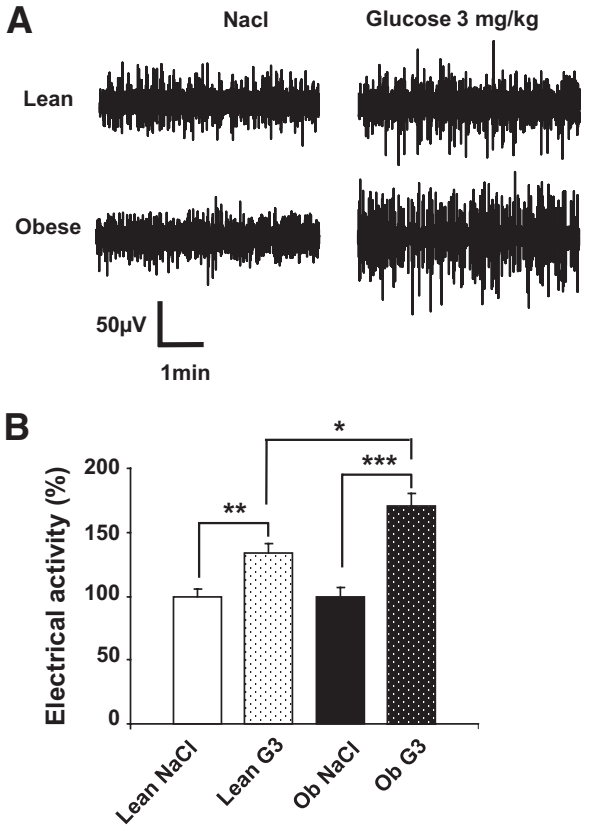

FIG. 3. Increased hypothalamic electrical activity in response to the low glucose dose. *A*: Multiunit sample recordings of arcuate nucleus neuronal activity in lean and obese Zücker rats after the carotid injection of saline (Nacl) or 3 mg/kg glucose (G3). *B*: Quantification of multiunit activity recorded in arcuate nucleus. Data are expressed as means ± SE corresponding to the percentage of the number of spikes measured in lean rats injected with saline. The bar graph depicts the electrical activity during the first minute after carotid injection of saline (NaCl) or 3 mg/kg glucose (G3) in lean (white bar) and in obese (Ob) rats (black bar). Asterisks indicate significant differences according to the unpaired Student's *t* test ($n = 6$ per genotype) (*$P < 0.05$, **$P < 0.01$, and ***$P < 0.0001$).

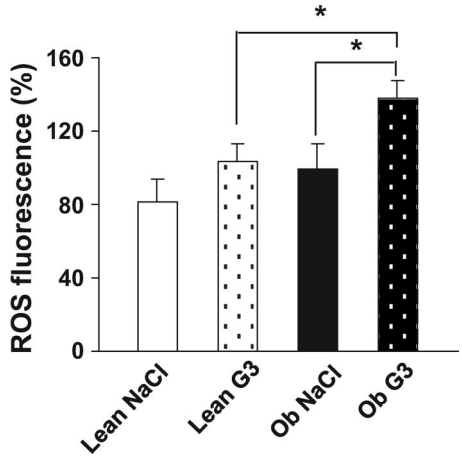

FIG. 4. Hypothalamic ROS production of obese rats in response to the low glucose load. ROS production in the hypothalamus in response to saline (NaCl) or to 3 mg/kg glucose (G3) injection toward the brain measured in lean (white bar) and in obese (Ob) rats (black bar). ROS level assessed in hypothalamic area by oxidation of dichlorofluorescein diacetate probe 1 min after intracarotid injection. Data are expressed as means ± SE (percentage of the ROS fluorescence observed in obese rats injected with saline). Asterisk indicates significant differences according to the post hoc Newman-Keuls test ($n = 8$–11 per genotype) (*$P < 0.05$).

Obese rats exhibit hypothalamic ROS production in response to the low glucose load. We measured ROS levels after saline or glucose injection. For this purpose, rats were injected through the carotid artery toward the brain with either the low dose of glucose or saline and killed 1 min after the injection (when insulin secretion occurs). ROS levels were assessed in both hypothalamus and thalamus. Interestingly, the basal constitutive ROS level, that is, assessed after saline intracarotid injection, was similar in both genotypes (Fig. 4). Glucose stimulation did not induce a significant change in hypothalamic ROS levels in lean rats. However, ROS levels were significantly increased (37%, $P < 0.05$) in obese rats injected with 3 mg/kg glucose when compared either with obese animals injected with saline or with lean rats injected with the same glucose load ($P < 0.05$, Fig. 4). Thus, low glucose stimulation mediates an increase in ROS levels only in obese rats. No such increase in ROS levels was found in thalamus, suggesting a regional specificity for this response (Fig. S1*A*, available in an online appendix at http://diabetes.diabetesjournals.org/cgi/content/full/db09-0110/DC1).

Abnormal ROS signaling is correlated to an alteration in the hypothalamic redox state. ROS level results from the balance between ROS production and detoxification. We measured enzymatic and nonenzymatic antioxidants in basal conditions (i.e., without glucose stimulation). The glutathione redox state, defined as GSSG-to-GSx ratio, as it is the major antioxidant that scavenges ROS, was oxidized twofold ($P < 0.001$) more in the hypothalamus of obese rats (Fig. 5*A*). Glutathione peroxidase activity was found to be significantly lower in the hypothalamus of obese rats (266.0 ± 28.7 vs. 166.0 ± 21.5; $P < 0.01$ in lean vs. obese rats) (Fig. 5*B*). Glutathione peroxidase activity did not vary in the thalamus (Fig. S1*B*). The mitochondrial MnSOD activity was also decreased in obese rats (0.0102 ± 0.0009 vs. 0.0065 ± 0.0008 enzymatic unit per milligrams proteins; $P < 0.01$ in lean vs. obese rats) whereas extramitochondrial CuZnSOD was not statistically different between the two genotypes (Fig. 5*C* and *D*). This strongly suggests a mitochondrial defect in antioxidant enzyme activity in the hypothalamus of obese rats. This is reinforced by the activity of aconitase, an enzyme of the Krebs's cycle sensitive to mROS and thus revealing the intramitochondrial redox state (31). This activity was significantly decreased (−39%; $P < 0.001$) in the hypothalamus of obese Zücker rats (Fig. 5*E*). Altogether, these results demonstrate that the hypothalamic redox state is lower in obese rats than in lean rats, regardless of the intracellular compartment studied.

Hypothalamic mitochondria exhibit increased activity in response to substrates. We explored the cytochrome c oxidase activity (cyclooxygenase [COX], complex IV), which reflects the oxidative potential of the mitochondrial respiratory chain. COX activity was significantly increased (51%; $P < 0.01$) in the hypothalamus of obese Zücker rats (Fig. 6*A*). To get further insight into the hypothalamic mitochondrial function, oxygen consumption by the electron transport chain was explored on isolated mitochondria (Fig. 6*B*). We performed titrations with glutamate (1, 5, and 20 mmol/l) to determine substrate-driven respiration. We highlighted a greater increase in the O_2 flux in response to glutamate in obese rats compared with lean ones. This increase was significant for each dose of glutamate (O_2 flux in lean vs. obese rats: 1 mmol/l,

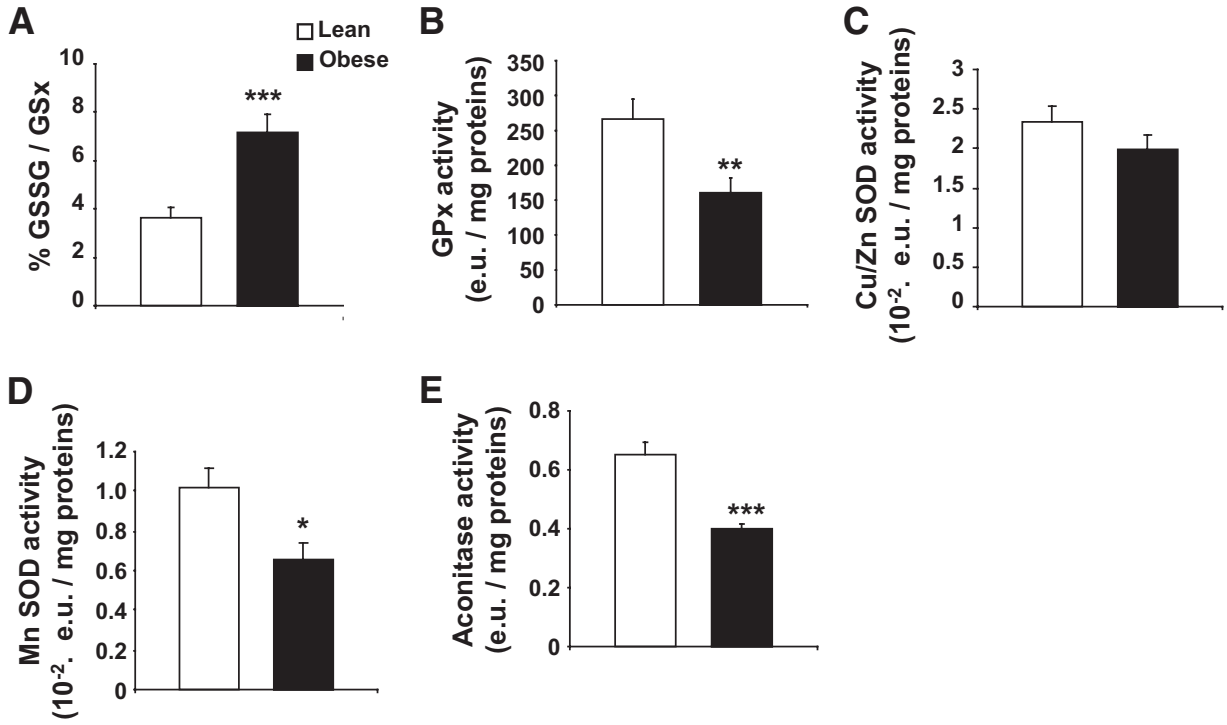

FIG. 5. Increased ROS production is linked to abnormal hypothalamic redox state. *A*: Obese rats display an abnormal hypothalamic glutathione redox state. GSH and GSSG levels measured by HPLC in hypothalamic homogenates of lean (white bar) and obese rats (black bar). The redox state of glutathione was calculated as the (GSSG/GSx) × 100. Asterisk indicates a significant difference according to the unpaired Student's *t* test ($n = 6$ per genotype) (*$P < 0.001$). *B*: Obese rats present a decrease in glutathione peroxidase activity. GPx activity measured in the hypothalamus of lean (white bar) and obese (black bar) rats (enzymatic units [e.u.]). Asterisk indicates a significant difference according to the unpaired Student's *t* test ($n = 6$ per genotype) (**$P < 0.01$). *C*: Obese rats present no difference in extramitochondrial Cu/Zn SOD activity. SOD activity measured in the hypothalamus of lean (white bar) and obese (black bar) rats (enzymatic units). No differences according to the unpaired Student's *t* test ($n = 6$ per genotype) were present. *D*: Obese rats present a decrease in mitochondrial MnSOD activity. Mitochondrial MnSOD activity measured in the hypothalamus of lean (white bar) and obese (black bar) rats (enzymatic units). Asterisk indicates a significant difference according to the unpaired Student's *t* test ($n = 6$ per genotype) (*$P < 0.05$). *E*: Obese rats show a decreased activity of the ROS-sensitive mitochondrial aconitase. Maximal aconitase activity measured in the hypothalamus of lean (white bar) and obese (black bar) rats (enzymatic units). Asterisk indicates a significant difference according to the unpaired Student's *t* test ($n = 6$ per genotype) (***$P < 0.001$).**

2.54 ± 1.03 vs. 6.34 ± 0.56 pmol/[s × mg], $P < 0.05$; 5 mmol/l, 4.70 ± 1.54 vs. 11.63 ± 2.30 pmol/[s × mg], $P < 0.05$; and 20 mmol/l, 7.81 ± 1.38 vs. 20.23 ± 5.57 pmol/[s × mg], $P < 0.05$), revealing a hypersensitivity to this substrate at the level of the respiratory chain. State 3 (substrates/ADP-driven) respiration was assessed with saturating ADP concentration. The O_2 flux 13.25 ± 2.43 pmol/(s × mg) versus 28.67 ± 5.69 pmol/(s × mg) in lean and obese rats, respectively, was increased in obese rats ($P < 0.05$). CAtr, an ATP-ADP exchange inhibitor, was then added to obtain the ADP-independent resting state 4, whereas respiration is only driven by substrates. State 4 was significantly enhanced in obese rats. Finally, the RCR (RCR = state 3/state 4) in lean rats (1.50 ± 0.52) was not significantly different from obese rats (1.50 ± 0.19). The total respiratory capacity induced by CCCP was significantly increased in obese rats (36.43 ± 1.00 pmol/[s × mg]) compared with lean ones (28.80 ± 2.44 pmol/[s × mg]), $P < 0.05$ (Fig. 6*C*). Next, we examined uncoupling respiration. Stimulation of uncoupling proteins with 300 μmol/l palmitate (Palm) did not reveal differences between lean (25.39 ± 2.17 pmol/[s × mg]) and obese (27.83 ± 3.86 pmol/[s × mg]) rats (Fig. 6*D*). This result reveals no difference in uncoupling respiration. In conclusion, these results indicate an increase in hypothalamic mitochondria activity at the complex I and IV, as revealed with glutamate assay and COX activity measurement. The increase in total respiratory capacity further supports these data. No difference was found regarding these parameters in the thalamus (Fig. S1*C–E*).

Expression of the five complexes of the respiratory chain was examined. Both nuclear (30 kDa subunit of complex II, core protein 2 subunit of complex III, and the α subunit of complex V) and mitochondrial (ND6 subunit of complex I and subunit 1 of complex IV) complexes encoded were quantified at the protein level by Western blotting (Fig. 6*E*). The expression of complexes I, II, III, and IV (COX) was increased in hypothalamic mitochondria from obese rats (177, 153, 128, and 159%). Complex V expression (105%) was unchanged (Fig. 6*F*). These results indicate an increased quantity of most complexes of the electron transport chain in the mitochondria of obese rats.

These differences were not caused by a change in mitochondrial number because citrate synthase activity was identical in both genotypes (Fig. 6*G*).

Restoration of hypothalamic redox state normalizes the response to glucose load in obese rats. We decided to normalize the glutathione redox state in obese rats to test whether this could explain impaired ROS production stimulated by the low glucose load (3 mg/kg). Therefore, reduced glutathione (GSH) was intracerebroventricularly infused over 3 days using an osmotic minipump. Well-being of the animals (weight gain and food intake) was preserved during the infusion (Fig. S2*A* and *B*). HPLC analysis revealed that the GSH chronic intracerebroventricular infusion was efficient to restore GSH redox state

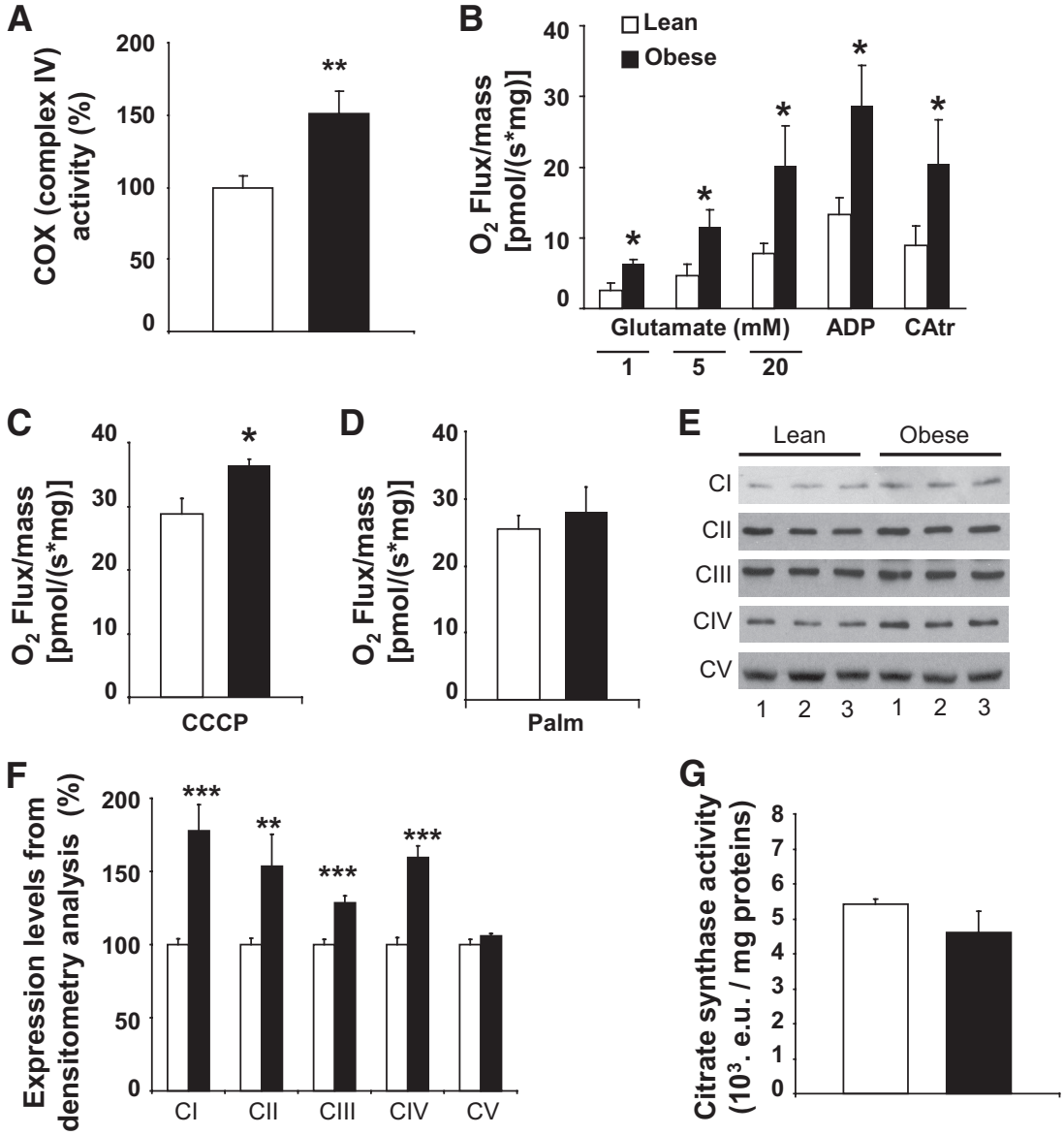

FIG. 6. Functional study of hypothalamic mitochondria. *A*: Obese rats exhibit an increased oxidative potential of the respiratory chain. Maximal cytochrome c oxidase activity in hypothalamic homogenates in basal conditions was significantly increased in obese rats. Data are expressed as means ± SE corresponding to the percentage of COX activity in lean rats. Asterisk indicates significant difference according to the unpaired Student's *t* test (n = 9–10 per genotype) ($P < 0.01$). *B*: Obese rats' mitochondria display a hypersensitivity to glutamate. Pharmacological settings for oxygraphic analysis on isolated hypothalamic mitochondria: glutamate titration (1, 5, and 20 mmol/l) to achieve the nonphosphorylating respiration; saturating ADP concentration to achieve state 3 respiration; full inhibition of ATP-synthase by CAtr gives state 4 respiration. Single comparisons were performed using the unpaired Student's *t* test to compare lean vs. obese rats. Asterisk indicates significant difference (*$P < 0.05$). *C*: Obese rats' mitochondria exhibit an enhanced maximal respiration capacity. Maximal respiration induced by CCCP (0.4 μmol/l). Asterisk indicates significant difference according to the Mann-Whitney *U* test (n = 6–8 per genotype) (*$P < 0.05$). *D*: Obese rats' mitochondria exhibit no uncoupling respiration. Uncoupling protein activation induced by palmitate (Palm) (300 μmol/l). No differences according to the unpaired Student's *t* test (n = 6 per genotype) were present. *E* and *F*: Overexpression of respiratory chain complexes I to IV in the hypothalamic mitochondria of obese rats. Western blot performed on isolated hypothalamic mitochondria. Immunoblots were quantified by densitometry analysis. Asterisk indicates significant differences according to the Mann-Whitney *U* test (n = 6–8 per genotype) (**$P < 0.01$ and ***$P < 0.001$). *G*: No difference in mitochondrial content. Mitochondrial content assessed by citrate synthase activity in the hypothalamus of lean (white bar) and obese (black bar) rats (enzymatic units [e.u.]). No differences according to the unpaired Student's *t* test (n = 6 per genotype) were present.**

within the hypothalami of obese rats (Fig. 7*A*). In contrast, it did not reverse mitochondrial function as measured on glutamate titration by oxygraphy (Fig. 7*B*). ROS levels and pancreatic insulin secretion were measured after the intracarotid 3 mg/kg glucose injection in glutathione-infused obese rats. Obese glutathione-infused rats did not have any more exacerbated ROS levels in response to the low glucose load and exhibited ROS levels similar to those of normal rats (Fig. 7*C*). Regarding the insulin response, it showed a full restoration of their sensitivity to glucose because their insulin peak was completely abolished in response to 3 mg/kg glucose. This result indicates a master role of mROS levels in response to glucose, at least for the nervous control of insulin secretion (Fig. 7*D*).

DISCUSSION

It has recently been demonstrated that glucose sensing was triggered by an intracellular redox signaling pathway in physiological conditions in the pancreas as well as in

A

Zücker	Lean	Obese	Obese GSH-infused
% GSSG / GSx	3.63 ± 0.44 (**)	7.16 ± 0.72	3.43 ± 0.37 (**)

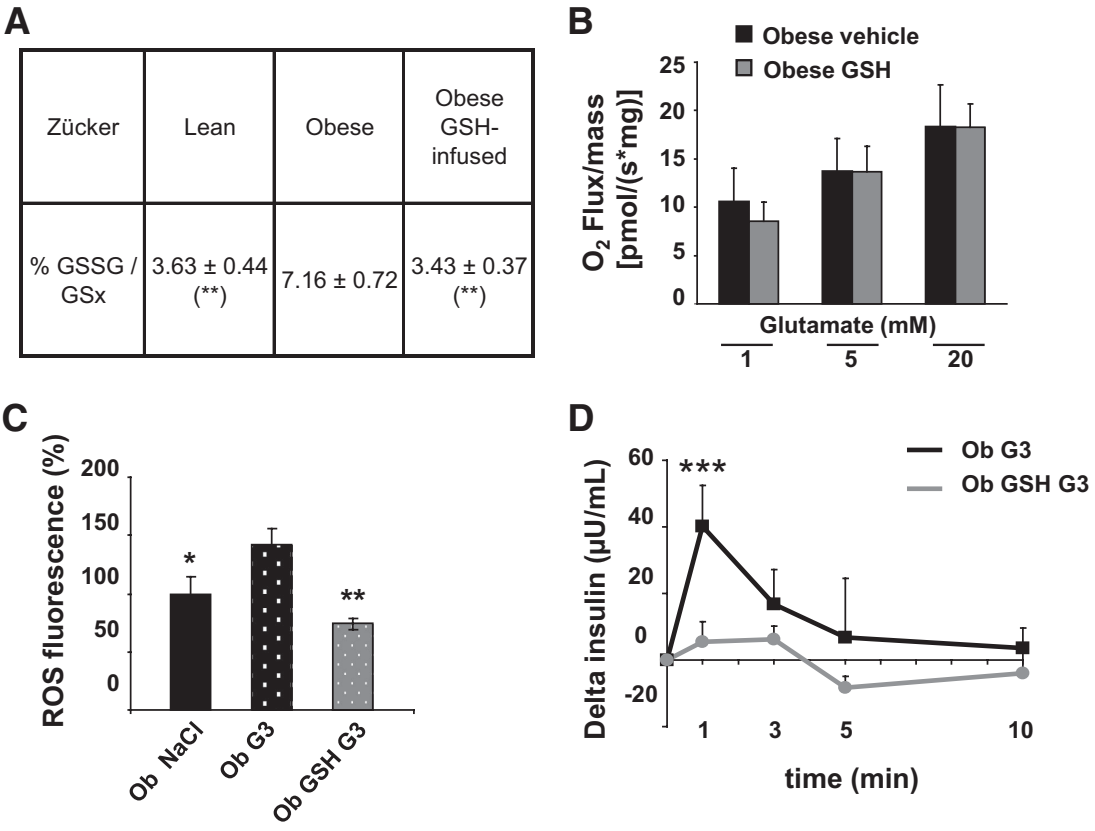

FIG. 7. Hypothalamic redox state after 3 days of intracerebroventricular GSH infusion in obese rats normalizes the response to the low glucose load. *A*: Normalization of the hypothalamic redox state. GSH and GSSG levels measured by HPLC in hypothalamic homogenates. The redox state of glutathione was calculated as (GSSG/GSx) × 100. Results are expressed as means ± SE of the glutathione redox state. Asterisk indicates significant difference according to the unpaired Student's *t* test ($n = 5–6$ per genotype) ($P < 0.01$) compared with the obese group. *B*: No change in hypothalamic mitochondrial hypersensitivity to glutamate in obese glutathione restored rats. Glutamate titration (1, 5, and 20 mmol/l) in obese GSH-restored rats (gray bar) did not differ from the vehicle-treated obese rats (black bar). No significant differences present according to the repeated-measures ANOVA analysis ($n = 4–6$) ($P_{anova} = 0.1576$). *C*: Normalization of hypothalamic ROS production. ROS production measured in obese rats after vehicle intracerebroventricular infusion and saline carotid injection (Ob NaCl, black bar [$n = 2$]), vehicle intracerebroventricular infusion and 3 mg/kg glucose carotid injection (Ob G3, dotted black bar [$n = 2$]), or GSH intracerebroventricular infusion and 3 mg/kg glucose carotid injection (Ob GSH G3, dotted gray bar [$n = 7$]). ROS levels were assessed on hypothalamic homogenates with the dichlorofluorescein diacetate probe 1 min after carotid injection. Data are expressed as means ± SE of the percentage of ROS fluorescence of the obese rats receiving the vehicle intracerebroventricular and saline carotid injection. Asterisk indicates significant differences according to the Newman-Keuls test ($n = 5–6$ per genotype) compared with the obese G3 group (*$P < 0.05$ and **$P < 0.01$). *D*: Normalization of insulin secretion. Plasma insulin assessed in obese rats in response to 3 mg/kg glucose injection toward the brain (black) and in obese GSH-infused rats in response to 3 mg/kg glucose (gray). Results are expressed as means ± SE corresponding to Δ from basal insulinemia at $t = 0$. Asterisk indicates significant differences according to independent statistical analysis using Mann-Whitney *U* test at $t = 1$ min ($n = 5–6$ per genotype) (***$P < 0.001$).**

the hypothalamus (11,12). However, the relevance of such a mechanism in metabolic disease is not known. We hypothesized that an alteration in redox signaling in the brain could participate in metabolic diseases. To test this hypothesis, we explored redox signaling in the Zücker rat. These rats are obese, insulin-resistant, and dyslipidemic but normoglycemic. One original feature of this model is its hypothalamic hypersensitivity to glucose (18). We specifically aimed to understand whether this hypersensitivity to glucose present in obese Zücker rats could be related to an alteration in redox signaling. For the first time, we revealed that this hypersensitivity was associated, within the hypothalamus, with *1*) an increased ROS level in response to the low glucose load, *2*) a constitutive oxidized environment at both the cellular and mitochondrial level, and *3*) an overexpression of several mitochondrial subunits of the respiratory chain, coupled with a global dysfunction in the mitochondrial activity. Moreover, pharmacological restoration of the hypothalamic redox state fully reversed the altered cerebral hypersensitivity to glucose. Altogether, these data suggest that this impaired metabolic regulation in the obese Zücker rat is linked to an abnormal redox signaling that originates from mitochondrial dysfunction.

In normal animals, hypothalamic glucose sensing promotes an increase in hypothalamic electrical activity and rapid and transient vagal-mediated insulin secretion (12,19). Moreover, we previously demonstrated that a key step in these events requires redox signaling because they were abolished when mROS were quenched (12). The hypersensitivity to glucose of obese Zücker rats has been demonstrated as an abnormal insulin response occurring after a low glucose load (3 vs. 9 mg/kg) that is inefficient in lean littermates (18). We confirmed this data regarding the peripheral insulin release and reinforced the notion of cerebral hypersensitivity to glucose in obese rats as assessed by the hypothalamic glucose-stimulated electrical activity. Indeed, we brought to light an increased level in the whole multicellular electrical activity in the arcuate nucleus of obese rats in response to 3 mg/kg glucose. Contrary to lean rats, this enhanced glucose-stimulated electrical activity was associated with the insulin response

in obese rats. This suggests that the electrical activity of the arcuate nucleus in response to 3 mg/kg glucose was high enough to promote insulin secretion in obese rats. Electrical activity was recorded under pentobarbital anesthesia that has depressive effects on nervous activity (32), thus suggesting a much greater effect on vigil rats. The multicellular recordings do not allow a distinction between direct versus presynaptic effects. However, numerous arcuate glucose-sensitive neurons have the ability to directly detect a change in glucose concentration (33). This cerebral hypersensitivity to glucose may explain the elevated parasympathetic tone that consequently contributes to the development of hyperinsulinemia in the obese Zücker rat (17,34).

In obese rats, there was a significant increase in ROS levels within the hypothalamus under low glucose stimulation at the time when plasma insulin increases. ROS concentration results from the balance between production and scavenging. The latter depends on the intracellular redox state (35,36). Glutathione redox (oxidized-to-total form ratio) constitutes an accurate indicator of the cellular redox state because glutathione is in large amount in cells (1–5 mmol/l) and considered as the major ROS detoxifying system (37). It has a pivotal and synergetic role with many other antioxidants by reducing pro-oxidant forms (36). In the hypothalamus of obese rats, glutathione was oxidized twofold more in basal conditions. Decreased GPx activity in the hypothalamus from obese rats further confirmed that basal redox state was deeply modified in this area. To gain insight into the oxidative environment in the mitochondria, we evaluated MnSOD and aconitase activity. MnSOD and aconitase, an enzyme involved in the Krebs cycle and sensitive to ROS, are exclusively located in the mitochondria (31). Their activities were decreased in the hypothalamus of the obese Zücker rat. In contrast, Cu/ZnSOD located in the cytosol did not vary. Altogether, these data reveal a constitutive oxidative environment in the hypothalamus of obese Zücker rats regardless of the intracellular compartment (cytosol or mitochondria). These results are in line with numerous studies showing a drop in the antioxidant defenses such as reduced glutathione, α-tocopherol, and catalase in several tissues of obese Zücker rats (38,39). Finally, the more oxidized cellular environment within the hypothalamus of obese rats could partly explain why an increased ROS level in response to the low glucose load is not buffered as in lean rats.

ROS are produced by electron leakage during mitochondrial metabolism, and the rate of their formation is enhanced as the mitochondrial metabolism increases (40–42). We explored the mitochondrial function in the hypothalamus of Zücker rats. First, the oxidative ability of the respiratory chain as determined by the cytochrome c oxidase activity, the total respiratory function as assessed with saturating substrate, and the chemical uncoupling were all significantly increased in the hypothalamus of obese rats. Second, the apparent affinity of the mitochondrial respiration for substrate was higher in obese rats as assessed by glutamate titration. Third, altered expression of mitochondrial complexes (I to IV) was increased in obese rats. These results are consistent with previous studies showing an increased oxidative capacity in the muscle of such rats, associated with an increasing number of functional units in the mitochondrial respiratory chain (43,44). No change in mitochondrial number was observed in the hypothalamus of obese rats as revealed by citrate synthase activity assay. Furthermore, it may be stressed that all these alterations are specific to the hypothalamus because no change was observed in the thalamus. Taken together with the absence of complex V modifications, the alterations seen between complexes I to IV may result in an enhancement in respiratory chain constraints (45). As an improved mitochondrial metabolism promotes ROS production under stimulation, this could represent the molecular basis of the abnormal increased ROS levels within the hypothalamus of obese rats in response to a low glucose load, in concert with the higher oxidized environment. One can speculate that the excessive mitochondrial ROS production might be a primary and causal link with the overoxidation of the redox state.

Recent observations from our laboratory and others (12,15,46) argue that ROS are part of hypothalamic activity control for the regulation of energy homeostasis. To date, ROS have been proposed as messengers in brain glucose and lipid sensing (12,46). For example, fasting abolished increased ROS in brain lipid sensing by increasing hypothalamic mitochondrial uncoupling (46); ghrelin signals are ROS-dependently integrated in NPY/AgRP neurons (15). Moreover, this latest study suggests that ROS signaling takes place in the neuronal population, although other cell types remain to be explored.

Here we show for the first time that dysfunction in hypothalamic redox signaling could be the molecular basis for impaired brain glucose sensing and might explain some features of the metabolic defects in obese rats such as hyperinsulinism. This has been strengthened by the experiment using a pharmacological approach (GSH treatment) that normalized the glutathione redox state. Indeed, such normalization reversed the increased ROS level as well as peripheral insulin secretion in response to a low glucose load (3 mg/kg). These findings highlight the necessity for a fine and balanced level of ROS dependent on the mitochondrial metabolism and the redox environment, which is required to trigger the appropriate redox signaling in response to glucose.

In summary, we demonstrated that the cerebral hypersensitivity to glucose in obese rats results from both impaired redox signaling and increased mitochondrial respiratory chain activity that lead to excessive ROS levels. One can postulate that these increased ROS levels activate redox signaling involving ROS-sensitive voltage-dependent channels (47,48). Changes in channel conformation will then modulate electrical activity that in turn triggers vagal-mediated insulin secretion. To determine whether hypothalamic mitochondrial dysfunction is of primary importance in the etiology of the hyperinsulinism in obesity, long-term treatment aiming to normalize redox state would provide interesting clues.

ACKNOWLEDGMENTS

This work was supported by grants from the Agence Nationale pour la Recherche (Nutrisens 05-PNRA-004) and from the Programme National de Recherche sur le Diabète (PNRD-0602).

No potential conflicts of interest relevant to this article were reported.

We fully acknowledge Jésus Garcia for his help in statistical analysis and the expertise of the Zootechnic Platform of the IFR31 Institute, I2MR, especially Christine Fourreau.

REFERENCES

1. Levin BE. Metabolic sensing neurons and the control of energy homeostasis. Physiol Behav 2006;89:486–489
2. Sandoval D, Cota D, Seeley RJ. The integrative role of CNS fuel-sensing mechanisms in energy balance and glucose regulation. Annu Rev Physiol 2008;70:513–535
3. Goldstone AP. The hypothalamus, hormones, and hunger: alterations in human obesity and illness. Prog Brain Res 2006;153:57–73
4. Schwartz MW, Porte D, Jr. Diabetes, obesity, and the brain. Science 2005;307:375–379
5. Penicaud L, Leloup C, Fioramonti X, Lorsignol A, Benani A. Brain glucose sensing: a subtle mechanism. Curr Opin Clin Nutr Metab Care 2006;9:458–462
6. Parton LE, Ye CP, Coppari R, Enriori PJ, Choi B, Zhang CY, Xu C, Vianna CR, Balthasar N, Lee CE, Elmquist JK, Cowley MA, Lowell BB. Glucose sensing by POMC neurons regulates glucose homeostasis and is impaired in obesity. Nature 2007;449:228–232
7. Yang XJ, Kow LM, Funabashi T, Mobbs CV. Hypothalamic glucose sensor: similarities to and differences from pancreatic β-cell mechanisms. Diabetes 1999;48:1763–1772
8. Kang L, Routh VH, Kuzhikandathil EV, Gaspers LD, Levin BE. Physiological and molecular characteristics of rat hypothalamic ventromedial nucleus glucosensing neurons. Diabetes 2004;53:549–559
9. Leloup C, Arluison M, Lepetit N, Cartier N, Marfaing-Jallat P, Ferre P, Penicaud L. Glucose transporter 2 (GLUT2): expression in specific brain nuclei. Brain Res 1994;638:221–226
10. Leloup C, Orosco M, Serradas P, Nicolaidis S, Penicaud L. Specific inhibition of GLUT2 in arcuate nucleus by antisense oligonucleotides suppresses nervous control of insulin secretion. Brain Res Mol Brain Res 1998;57:275–280
11. Pi J, Bai Y, Zhang Q, Wong V, Floering LM, Daniel K, Reece JM, Deeney JT, Andersen ME, Corkey BE, Collins S. Reactive oxygen species as a signal in glucose-stimulated insulin secretion. Diabetes 2007;56:1783–1791
12. Leloup C, Magnan C, Benani A, Bonnet E, Alquier T, Offer G, Carriere A, Periquet A, Fernandez Y, Ktorza A, Casteilla L, Penicaud L. Mitochondrial reactive oxygen species are required for hypothalamic glucose sensing. Diabetes 2006;55:2084–2090
13. Leloup C, Tourrel-Cuzin C, Magnan C, Karaca M, Castel J, Carneiro L, Colombani AL, Ktorza A, Casteilla L, Penicaud L. Mitochondrial reactive oxygen species are obligatory signals for glucose-induced insulin secretion. Diabetes 2009;58:673–681
14. Levin BE, Magnan C, Migrenne S, Chua SC, Jr, Dunn-Meynell AA. F-DIO obesity-prone rat is insulin resistant before obesity onset. Am J Physiol Regul Integr Comp Physiol 2005;289:R704–R711
15. Andrews ZB, Liu ZW, Walllingford N, Erion DM, Borok E, Friedman JM, Tschop MH, Shanabrough M, Cline G, Shulman GI, Coppola A, Gao XB, Horvath TL, Diano S. UCP2 mediates ghrelin's action on NPY/AgRP neurons by lowering free radicals. Nature 2008;454:846–851
16. York DA, Marchington D, Holt SJ, Allars J. Regulation of sympathetic activity in lean and obese Zucker (*fa/fa*) rats. Am J Physiol 1985;249:E299–E305
17. Penicaud L, Cousin B, Leloup C, Atef N, Casteilla L, Ktorza A. Changes in autonomic nervous system activity and consecutive hyperinsulinaemia: respective roles in the development of obesity in rodents. Diabete Metab 1996;22:15–24
18. Alquier T, Leloup C, Atef N, Fioramonti X, Lorsignol A, Penicaud L. Cerebral insulin increases brain response to glucose. J Neuroendocrinol 2003;15:75–79
19. Atef N, Ktorza A, Penicaud L. CNS involvement in the glucose induced increase of islet blood flow in obese Zucker rats. Int J Obes Relat Metab Disord 1995;19:103–107
20. Wang R, Cruciani-Guglielmacci C, Migrenne S, Magnan C, Cotero VE, Routh VH. Effects of oleic acid on distinct populations of neurons in the hypothalamic arcuate nucleus are dependent on extracellular glucose levels. J Neurophysiol 2006;95:1491–1498
21. Anderson MF, Nilsson M, Eriksson PS, Sims NR. Glutathione monoethyl ester provides neuroprotection in a rat model of stroke. Neurosci Lett 2004;354:163–165
22. Benani A, Barquissau V, Carneiro L, Salin B, Colombani AL, Leloup C, Casteilla L, Rigoulet M, Penicaud L. Method for functional study of mitochondria in rat hypothalamus. J Neurosci Methods 2009;178:301–307
23. Szabados E, Fischer GM, Toth K, Csete B, Nemeti B, Trombitas K, Habon T, Endrei D, Sumegi B. Role of reactive oxygen species and poly-ADP-ribose polymerase in the development of AZT-induced cardiomyopathy in rat. Free Radic Biol Med 1999;26:309–317
24. Zheng W, Ren S, Graziano JH. Manganese inhibits mitochondrial aconitase: a mechanism of manganese neurotoxicity. Brain Res 1998;799:334–342
25. Galinier A, Carriere A, Fernandez Y, Caspar-Bauguil S, Periquet B, Periquet A, Penicaud L, Casteilla L. Site specific changes of redox metabolism in adipose tissue of obese Zucker rats. FEBS Lett 2006;580:6391–6398
26. Marklund S, Marklund G. Involvement of the superoxide anion radical in the autoxidation of pyrogallol and a convenient assay for superoxide dismutase. Eur J Biochem 1974;47:469–474
27. Gunzler WA, Kremers H, Flohe L. An improved coupled test procedure for glutathione peroxidase (EC 1-11-1-9-) in blood. Z Klin Chem Klin Biochem 1974;12:444–448
28. Faloona GR, Srere PA. Escherichia coli citrate synthase. Purification and the effect of potassium on some properties. Biochemistry 1969;8:4497–4503
29. Prunet-Marcassus B, Moulin K, Carmona MC, Villarroya F, Penicaud L, Casteilla L. Inverse distribution of uncoupling proteins expression and oxidative capacity in mature adipocytes and stromal-vascular fractions of rat white and brown adipose tissues. FEBS Lett 1999;464:184–188
30. Guillod-Maximin E, Lorsignol A, Alquier T, Penicaud L. Acute intracarotid glucose injection towards the brain induces specific c-fos activation in hypothalamic nuclei: involvement of astrocytes in cerebral glucose-sensing in rats. J Neuroendocrinol 2004;16:464–471
31. Tretter L, Adam-Vizi V. α-ketoglutarate dehydrogenase: a target and generator of oxidative stress. Philos Trans R Soc Lond B Biol Sci 2005;360:2335–2345
32. Kitahara S, Yamashita M, Ikemoto Y. Effects of pentobarbital on purinergic P2X receptors of rat dorsal root ganglion neurons. Can J Physiol Pharmacol 2003;81:1085–1091
33. Fioramonti X, Lorsignol A, Taupignon A, Penicaud L. A new ATP-sensitive K^+ channel-independent mechanism is involved in glucose-excited neurons of mouse arcuate nucleus. Diabetes 2004;53:2767–2775
34. Rohner-Jeanrenaud F, Hochstrasser AC, Jeanrenaud B. Hyperinsulinemia of preobese and obese *fa/fa* rats is partly vagus nerve mediated. Am J Physiol 1983;244:E317–E322
35. Valko M, Leibfritz D, Moncol J, Cronin MT, Mazur M, Telser J. Free radicals and antioxidants in normal physiological functions and human disease. Int J Biochem Cell Biol 2007;39:44–84
36. Nordberg J, Arner ES. Reactive oxygen species, antioxidants, and the mammalian thioredoxin system. Free Radic Biol Med 2001;31:1287–1312
37. Wu G, Fang YZ, Yang S, Lupton JR, Turner ND. Glutathione metabolism and its implications for health. J Nutr 2004;134:489–492
38. Soltys K, Dikdan G, Koneru B. Oxidative stress in fatty livers of obese Zucker rats: rapid amelioration and improved tolerance to warm ischemia with tocopherol. Hepatology 2001;34:13–18
39. Poirier B, Lannaud-Bournoville M, Conti M, Bazin R, Michel O, Bariety J, Chevalier J, Myara I. Oxidative stress occurs in absence of hyperglycaemia and inflammation in the onset of kidney lesions in normotensive obese rats. Nephrol Dial Transplant 2000;15:467–476
40. Brownlee M. The pathobiology of diabetic complications: a unifying mechanism. Diabetes 2005;54:1615–1625
41. Nishikawa T, Edelstein D, Du XL, Yamagishi S, Matsumura T, Kaneda Y, Yorek MA, Beebe D, Oates PJ, Hammes HP, Giardino I, Brownlee M. Normalizing mitochondrial superoxide production blocks three pathways of hyperglycaemic damage. Nature 2000;404:787–790
42. Yamagishi SI, Edelstein D, Du XL, Brownlee M. Hyperglycemia potentiates collagen-induced platelet activation through mitochondrial superoxide overproduction. Diabetes 2001;50:1491–1494
43. Turner N, Bruce CR, Beale SM, Hoehn KL, So T, Rolph MS, Cooney GJ. Excess lipid availability increases mitochondrial fatty acid oxidative capacity in muscle: evidence against a role for reduced fatty acid oxidation in lipid-induced insulin resistance in rodents. Diabetes 2007;56:2085–2092
44. Bonnard C, Durand A, Peyrol S, Chanseaume E, Chauvin MA, Morio B, Vidal H, Rieusset J. Mitochondrial dysfunction results from oxidative stress in the skeletal muscle of diet-induced insulin-resistant mice. J Clin Invest 2008;118:789–800
45. Adam-Vizi V, Chinopoulos C. Bioenergetics and the formation of mitochondrial reactive oxygen species. Trends Pharmacol Sci 2006;27:639–645
46. Benani A, Troy S, Carmona MC, Fioramonti X, Lorsignol A, Leloup C, Casteilla L, Penicaud L. Role for mitochondrial reactive oxygen species in brain lipid sensing: redox regulation of food intake. Diabetes 2007;56:152–160
47. Hudasek K, Brown ST, Fearon IM. H_2O_2 regulates recombinant Ca^{2+} channel α-1C subunits but does not mediate their sensitivity to acute hypoxia. Biochem Biophys Res Commun 2004;318:135–141
48. Avshalumov MV, Chen BT, Koos T, Tepper JM, Rice ME. Endogenous hydrogen peroxide regulates the excitability of midbrain dopamine neurons via ATP-sensitive potassium channels. J Neurosci 2005;25:4222–4231